

Optimization of Selective Inversion Recovery Magnetization Transfer Imaging for Clinical Applications

Richard D. Dortsch^{1,2}, Ke Li^{1,2}, Daniel F. Gochberg^{1,2}, John C. Gore^{1,2}, and Seth A. Smith^{1,2}

¹Radiology and Radiological Sciences, Vanderbilt University, Nashville, TN, United States, ²Vanderbilt University Institute of Imaging Science, Vanderbilt University, Nashville, TN, United States

Target Audience: Imaging scientists interested in quantitative myelin imaging methods and the White Matter Study Group of the ISMRM.

Purpose: To optimize a selective inversion recovery (SIR) quantitative magnetization transfer (qMT) protocol for efficient mapping of myelin content [1]. SIR is based upon the application of a low-power inversion pulse, which inverts water protons with minimal impact on macromolecular protons [2]. The resulting biexponential recovery is sampled at various inversion times (TI) to estimate: 1) the macromolecular to free proton pool-size-ratio ($PSR = M_{0m}/M_{0f}$), 2) the rate of MT from free to macromolecular pools ($k_{mf} = k_{fm}/PSR$), 3) the R_1 of the free pool (R_{1f}), 4) the size of the free pool (M_{0f}), and 5) the free pool inversion efficiency (S_f). Previous work [3] has shown that efficient SIR protocols can be achieved by varying the predelay time (TD = delay between spin-echo and next inversion pulse) in combination with TI. Here, we show that additional gains can be achieved by fixing k_{mf} during the fitting process. More specifically, we performed numerical studies to find optimal TI/TD values in terms of the precision and accuracy of qMT parameter estimates (PSR , R_{1f} , M_{0f} , and S_f); and these strategies were tested in phantoms and healthy human brains.

Methods: Numerical Optimizations: Optimizations were performed to find: 1) a 5-point scheme (k_{mf} = free parameter) and 2) a 4-point scheme ($k_{mf} = 12.5 \text{ s}^{-1}$ [4]). For a set of TI/TD values and qMT parameters, Cramér-Rao lower bound theory [5] was used to determine the mean-squared error [$\text{MSE} = (\text{bias}^2 + \text{precision}^2)$] efficiency of estimated qMT parameters (see [3,5] for details). TI/TD values that maximized MSE efficiency were found using a combination of genetic and sequential quadratic programming algorithms (`ga` and `fmincon`, MATLAB 2014b). All optimizations were performed over four sets of qMT parameters, covering the range of values observed in healthy and multiple sclerosis (MS) brains at 3.0 T [4]. To ensure adequate results in heterogeneous samples, the tissue yielding the lowest MSE efficiency (i.e., worst-case scenario) was selected at each step.

Data Acquisition: Bovine serum albumin (BSA: samples contained 5-20% BSA plus 0-0.05 mM MnCl_2) and four healthy volunteers (25–26 y.o.) were imaged using a 3.0-T Philips Achieva MR scanner. A two-channel body coil and a 32-channel head coil were used for excitation and reception, respectively. Single-slice SIR data were collected with TI/TD values from the optimizations above along with a 16-point scheme [4] for comparison (TI logarithmically spaced from 0.01-10 s and TD = 2.5 s). Additional parameters included: TSE factor = 26, echo spacing = 5.9 ms, TE = 80 ms, SENSE factor = 2.2, resolution = $2 \times 2 \times 5 \text{ mm}^3$, and two acquisitions. **Data Analysis:** SIR parameters were determined using the standard SIR analysis [3]. For the 4-point analysis, k_{mf} was fixed to published [4] mean values in each sample ($12.5 \text{ and } 35 \text{ s}^{-1}$ for brain and BSA, respectively).

Results and Discussion: Numerical Optimizations: Precise and accurate 5-point [TI = {10,50,56,277,843} and TD = {3270,4489,1652,2922,10} ms] and 4-point schemes [TI = {10,10,278,1007} and TD = {684,4171,2730,10} ms] were found. Relative to the 16-point scheme, simulations predict a $\approx 40\%$ and $\approx 80\%$ increase in the SNR efficiency of PSR for the 5- and 4-point schemes, respectively. **BSA Phantoms:** Fig. 1 shows fit PSR and R_{1f} values in BSA phantoms. The 5- and 4-point schemes yielded parameters at similar levels of precision (and no bias) relative to the 16-point scheme, but with $\approx 4x$ (40 sec/slice) and $\approx 6x$ (60 sec/slice) faster scan times, respectively. In addition, PSR was insensitive to T_1 (see MnCl_2 -doped samples). **Healthy Subjects:** Fig. 2 shows representative qMT parameter maps from a healthy subject. Once again, similar levels of precision were obtained in the optimized and 16-point schemes. Furthermore, although k_{mf} varied across the brain, 4-point parameter values showed little bias (mean PSR and R_{1f} values were 10% higher and 7% lower, respectively). Because similar levels of bias were observed in the 5-point data, we postulate that this is driven by incorrect model assumptions (e.g., from water compartment [6]) that may be accentuated when TD is varied. Finally, note the reduced sensitivity to CSF partial-volume averaging in the 4-point data (voxels with elevated $PSRs$, white arrow), which is due to fixing k_{mf} .

Conclusions: SIR parameters can be efficiently and accurately estimated from four optimized images. This efficiency will be exploited for clinical applications that require high-resolution (e.g., peripheral nerve) or large volumetric coverage. For example, 24 slices could be acquired in 8 minutes using the 4-point scheme (3D scan with 2x SENSE acceleration in the slice direction). Future work includes validating these protocols in pathology. We anticipate that this will be successful as: i) k_{mf} is relatively insensitive to pathology [7] and ii) our optimizations included data from MS lesions.

References: [1] Odrobina. *NMR Biomed* **18**: 277 (2005). [2] Edzes. *Nature* **254**: 521 (1977). [3] Li. *MRM* **64**: 491 (2010). [4] Dortsch. *MRM* **66**: 1346 (2011).

[5] Lankford. *MRM* **69**: 127 (2013). [6] Stanisz. *MRM* **42**: 1128 (1999). [7] Smith. *MRM* **61**: 22 (2009). **Acknowledgements:** K25 EB013659 for funding.

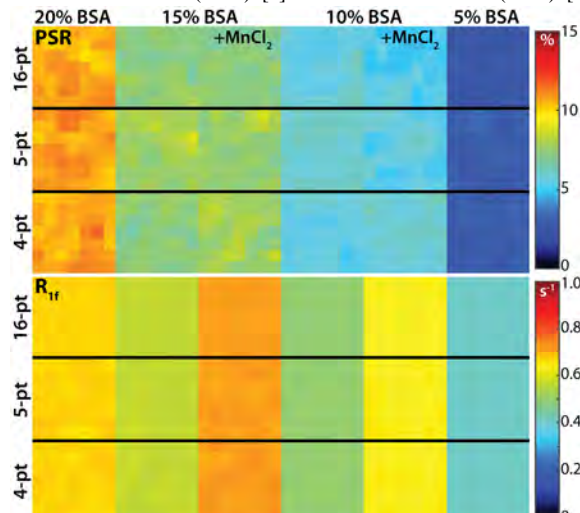


Fig 1. PSR (top) and R_{1f} (bottom) from the center 7×7 grid in each BSA phantom (left-to-right) using each sampling scheme (top-to-bottom).

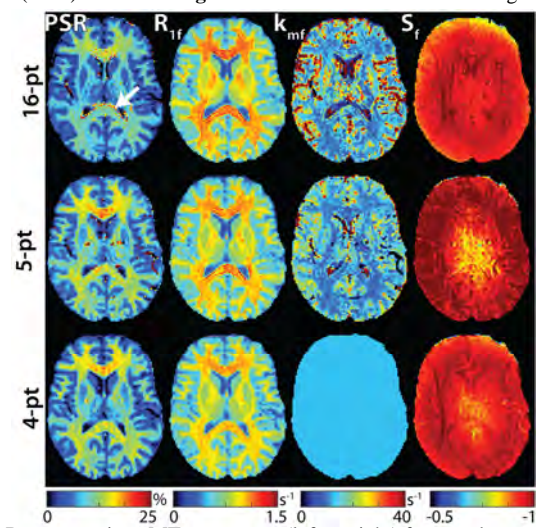


Fig 2. Representative qMT parameters (left-to-right) from each sampling scheme (top-to-bottom). Arrow denotes voxels corrupted via partial-voluming.